Published in IEEE TRANSACTIONS ON MEDICAL IMAGING, VOL. 24, NO. 5, p. 604-611, MAY 2005. Personal use of this material is permitted. However, permission to reprint/republish this material for advertising or promotional purposes or for creating new collective works for resale or redistribution to servers or lists, or to reuse any copyrighted component of this work in other works, must be obtained from IEEE TRANSACTIONS ON MEDICAL IMAGING.

Generalized Likelihood Ratio Tests for Complex fMRI Data: A Simulation Study

J. Sijbers* and A. J. den Dekker

***Abstract*—Statistical tests developed for the analysis of (intrinsically complex valued) functional magnetic resonance time series, are generally applied to the data's magnitude components. However, during the past five years, new tests were developed that incorporate the complex nature of fMRI data. In particular, a generalized likelihood ratio test (GLRT) was proposed based on a constant phase model [19]. In this work, we evaluate the sensitivity of GLRTs for complex data to small misspecifications of the phase model by means of simulation experiments. It is argued that, in practical situations, GLRTs based on magnitude data are likely to perform better compared to GLRTs based on complex data in terms of detection rate and constant false alarm rate properties.**

***Index Terms*—fMRI, generalized likelihood ratio test, magnitude data, statistical parametric maps.**

I. Introduction

MAGNETIC resonance imaging is not only capable of providing excellent anatomical information. It also offers the ability to visualize functional activity in the human brain, by means of so-called functional magnetic resonance imaging (fMRI). fMRI is a technique for determining which parts of the brain are activated by different types of stimuli. From a succession of rapidly acquired images that reflect localized changes in cerebral blood flow and oxygenation, fMRI can provide detailed images of localized brain activity induced by sensory, motor, or cognitive tasks, by processing each pixel's time series. Since activation-related signal changes are of the order of 1% to 10%, the construction of such activation maps requires sophisticated statistical tests.

In the past, many techniques were proposed for the construction of activation maps, often referred to as statistical parametric maps (SPMs). Initial detection methods were based on simple subtraction of images acquired during a resting state from images acquired during activation [1], [31]. In order to improve the detection rate, activation detection methods using the z-score, correlation coefficients, analysis of variance, or Student-t test statistics were employed [20], [23]. Those tests all fit into the framework of the so-called general linear model (GLM) test [5]. A main advancement of the GLM test was the incorporation of a hemodynamic response function. Furthermore, more flexible and general variants of the general linear model were developed such as tests based on independent component analysis [16], [27], multiresolution analysis [4], and likelihood ratio tests [19], [22].

Although magnetic resonance data are intrinsically complex valued, statistical tests are generally applied to magnitude fMRI images, since only the signal amplitude is assumed to be related to neural activation. Indeed, most of the tests available for fMRI data analysis were specifically developed for magnitude (i.e., single-valued) times series. Only recently, tests were developed for complex valued data [3], [19], [21]. In this respect, Nan and Nowak showed how to construct a generalized likelihood ratio test (GLRT) for complex fMRI data with constant phase values [19]. Thereby, it was shown that, under the assumption of a constant phase model, the GLRT has a significantly higher detection rate compared to tests based on magnitude data, especially in low signal-to-noise (SNR) regions.

The assumption of constant phases, however, is crucial and may be too restrictive. In this respect, it has previously been reported that phase traces may exhibit activation-dependent modulations, especially for voxels with large venous blood fractions (i.e., voxels with high blood volume fractions show a time-dependency related to the paradigm) [10], [17]. On the other hand, since in most fMRI studies, a voxel contains a large ensemble of vessels with various orientations and sizes, the assumption of a constant phase value may still be appropriate. However, there may also be other causes for nonconstant phases as a function of time. For example, due to physiological processes or instabilities of the MR imaging system, the phase may show a slowly varying drift [12]. Similar phase behavior was found in our experimental fMRI data sets: though most data sets show constant phase values as a function of time, some of those data sets clearly revealed linear phase drifts (e.g., see Fig. 1).

In this paper, we take a closer look at the feasibility of the constant phase assumption underlying the GLRT proposed by Nan and Nowak [19]. Thereby, we will try to answer questions like "What if the true phase values are not truly constant but, for example, are more appropriately described by a linear phase model?" and "Would it be helpful to construct a GLRT based on a more complex phase model, or should we rather apply a GLRT based on magnitude data?".

In order to simplify the discussion (as was also done by Nan and Nowak), the noise disturbing the fMRI time series is assumed to be Gaussian white noise [13], [15], [19]. The white noise model may be an oversimplification of the noises inherent in fMRI (especially if physiological noise is dominant

Manuscript received November 17, 2004; revised January 6, 2005. The Associate Editor responsible for coordinating the review of this paper and recommending its publication was P. M. Thompson. *Asterisk indicates corresponding author.*

*J. Sijbers is with the University of Antwerp, Vision Lab, CMI, Groenenborgerlaan 171, U316, B-2020 Antwerpen, Belgium and also with the Fund for Scientific Research-Flanders, Belgium (F.W.O.), Egmontstraat 5 1000 Brussels, Belgium (e-mail: jan.sijbers@ua.ac.be).

A. J. den Dekker is with the Delft University of Technology, Delft Center for Systems and Control, 2628CD Delft, The Netherlands (e-mail: a.j.den-dekker@dcsc.tudelft.nl).

Digital Object Identifier 10.1109/TMI.2005.844075

0278-0062/$20.00 © 2005 IEEE

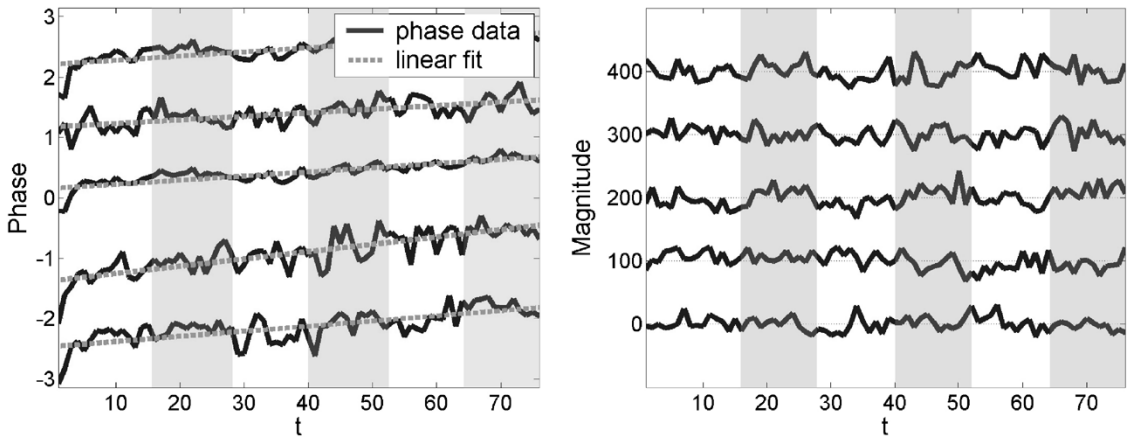

Fig. 1. Left: phase time courses of an experimental fMRI data set. The paradigm was four "dummy" images followed by a 12 rest—12 stimulus period, repeated three times (i.e., 76 images in total). Right: the magnitude traces corresponding to the phase traces on the left (the offset of each magnitude trace was adjusted for matching with the phase trace). No significant activation was detected in the magnitude traces, except for the middle trace (offset 200). For both plots, the task paradigm is shown in the background (gray denotes stimulus).

over thermal noise). However, if the data are observed to be correlated, they can be whitened based on an estimated autocorrelation structure [2], [19], [29]–[30]. Moreover, valuable methods exist to eliminate, for example, physiological noise from the fMRI time courses, prior to activation detection [3], [7], [28]. Hence, the conclusions of this work can easily be extended to more realistic noise models that incorporate colored noise.

The organization of this paper is as follows. Section II briefly reviews the general theory for the construction of a GLRT. In Section III, the GLRTs for magnitude as well as for complex data with a constant, linear, or random phase model are derived. Next, in Section IV, simulation experiments are discussed that were set up to test the performance of the GLRTs. Finally, conclusions are drawn in Section V.

II. A General Description of Generalized Likelihood Ratio Tests

In this section, the general theory for the construction of a GLRT for the class of hypothesis testing problems considered in this paper will be outlined. Let $\underline{\boldsymbol{w}} = (\underline{w}_1, \ldots, \underline{w}_N)^T$ be a random sample vector with joint probability density function (PDF) $p_{\underline{\boldsymbol{w}}}(\boldsymbol{x}; \boldsymbol{\theta})$, in which $\boldsymbol{\theta} = (\theta_1, \ldots, \theta_k)^T$ denotes the vector of unknown parameters and $\boldsymbol{x} = (x_1, \ldots, x_N)^T$ represents the vector of variables corresponding to the random sample vector $\underline{\boldsymbol{w}}$.[1] The superscript T denotes matrix transposition. Suppose that we wish to test the composite null hypothesis:

$$H_0 : \theta_1 = \theta_1^0, \cdots, \theta_r = \theta_r^0, \theta_{r+1}, \cdots, \theta_k \tag{1}$$

where $\theta_1^0, \ldots, \theta_r^0$ are known and $\theta_{r+1}, \ldots, \theta_k$ are left unspecified, against the alternative composite hypothesis H_1 under which all parameters $\theta_1, \ldots, \theta_k$ are left unspecified.

Next, suppose that we have a set of observations $\boldsymbol{w} = (w_1, \ldots, w_N)^T$, and that we substitute these observations for the corresponding variables $\boldsymbol{x}$ in the joint PDF of the random sample $\underline{\boldsymbol{w}}$. The resulting function is a function of the unknown parameter vector $\boldsymbol{\theta}$ only. By regarding these parameters as variables, the so called likelihood function $L(\boldsymbol{\theta}; \boldsymbol{w})$ is obtained. Then the generalized likelihood-ratio (GLR) λ is defined as follows [9], [18]:

$$\lambda \equiv \lambda(\boldsymbol{w}) = \frac{\sup_{\theta_1, \cdots, \theta_k} L(\theta_1, \cdots, \theta_k; \boldsymbol{w})}{\sup_{\theta_{r+1}, \cdots, \theta_k} L(\theta_1^0, \cdots, \theta_r^0, \theta_{r+1}, \cdots, \theta_k; \boldsymbol{w})}. \tag{2}$$

Note that λ is a function of the observations $\boldsymbol{w}$ only. If these observations are replaced by their corresponding random variables $\underline{\boldsymbol{w}}$, then we write $\underline{\lambda}$ for λ, that is, $\underline{\lambda} = \underline{\lambda}(\underline{\boldsymbol{w}})$. Since $\underline{\lambda}$ is a function of the random vector $\underline{\boldsymbol{w}}$, it is a random variable itself. In fact, $\underline{\lambda}$ is a statistic, since it does not depend on unknown parameters. Note that the denominator of $\underline{\lambda}$ is the likelihood function evaluated at the maximum likelihood (ML) estimator (MLE) under H_0, whereas the numerator of $\underline{\lambda}$ is the likelihood function evaluated at the ML estimator under H_1. The generalized likelihood ratio test principle now states that H_0 is to be rejected if and only if the sample value λ of $\underline{\lambda}$ satisfies the inequality $\lambda \geq \lambda_0$ where λ_0 is some user specified threshold.

It may sometimes be difficult to find the distribution of $\underline{\lambda}$, which is required to evaluate the power of the test [18]. However, it can be shown that, asymptotically (i.e., for $N \to \infty$), the modified GLR statistic $2 \ln \underline{\lambda}$ possesses a χ_r^2 distribution, that is, a chi-square distribution with r degrees of freedom, when H_0 is true. Furthermore, it can be shown that for the case of a linear model and Gaussian distributed noise, these asymptotic properties are exact, even for a finite number of observations [11]. Alternative modified GLRT statistics having a known distribution (under H_0) may be found. Knowledge of the PDF of the test statistic allows one to compose GLRTs with a desired *false alarm rate*. The false alarm rate is given by the probability that the test will decide H_1 when H_0 is true. The *detection rate* is given by the probability that the test will decide H_1 when H_1 is true. Throughout this paper, we will denote the false alarm rate and the detection rate by P_f and P_d, respectively. Furthermore, a test has the so-called constant false-alarm rate (CFAR) property if, independent of the SNR, the threshold that yields a constant P_f can be found. GLRTs will have the CFAR property at least

[1]Here and in what follows, random variables are underlined, small bold characters denote vectors, and capital bold characters denote matrices.

asymptotically since the asymptotic PDF of a GLRT is known and does not depend on any unknown parameters. Whether or not a GLRT has the CFAR property for a finite number of observations can be found out by means of simulations. For more details on the GLRT, see [11].

III. Methods

In this section, we describe the construction of various GLRTs for fMRI data. Thereby, we will consider the problem of testing whether the response of an fMRI data set $\boldsymbol{w} = (w_1, \ldots, w_N)^T$ of sample size N to a known reference function $\boldsymbol{r} = (r_1, \ldots, r_N)^T$ is significant. Without loss of generality, it is assumed that $\boldsymbol{r}^T.\mathbf{1} = 0$ and $\boldsymbol{r}^T.\boldsymbol{r} = N$, where $\mathbf{1}$ denotes an $N \times 1$ vector of ones. In addition, the noiseless magnitude data set is assumed to be described by the following $N \times 1$ deterministic signal vector:

$$\boldsymbol{z} = a\mathbf{1} + b\boldsymbol{r}. \tag{3}$$

Hence, $\boldsymbol{z}$ is a constant baseline with height a on which a reference function $\boldsymbol{r}$ with amplitude b is superimposed. The reference function may be, for example, a block function convolved with a hemodynamic response function. In the absence of activity, $b = 0$, so that $\boldsymbol{z} \equiv a\mathbf{1}$. We will consider the problem of testing the hypothesis that $b = 0 (H_0)$ against the hypothesis that $b \neq 0 (H_1)$.

A. GLRT for Magnitude fMRI Data

In this subsection, we describe the construction of a GLRT for a *magnitude* fMRI data set $\boldsymbol{m} = (m_1, \ldots, m_N)^T$. It is well known that magnitude data are Rician distributed (magnitude data are derived from complex valued data of which the components are Gaussian distributed). The Rician PDF of magnitude data with deterministic signal component z and noise variance σ^2, is given by [8]:

$$p_{\underline{m}}(x|z) = \frac{x}{\sigma^2} e^{-\frac{x^2+z^2}{2\sigma^2}} I_0\left(\frac{zx}{\sigma^2}\right) \tag{4}$$

where I_0 is the zeroth order modified Bessel function of the first kind. With increasing SNR (defined as z/σ), the Rician distribution tends to a Gaussian distribution [26].

1) *ML estimation under H_0*: The likelihood function under H_0 is given by

$$L(a, \sigma^2; \boldsymbol{m}) = \prod_{n=1}^{N} \frac{m_n}{\sigma^2} e^{-\frac{m_n^2+a^2}{2\sigma^2}} I_0\left(\frac{m_n a}{\sigma^2}\right). \tag{5}$$

Maximizing $\ln L$ with respect to (a, σ^2) yields the MLEs of a and σ^2 under H_0, denoted as $\widehat{\underline{a}}_0$ and $\widehat{\underline{\sigma}_0^2}$, respectively.

2) *ML estimation under H_1*: The likelihood function under H_1 is given by

$$L(a, b, \sigma^2; \boldsymbol{m}) = \prod_{n=1}^{N} \frac{m_n}{\sigma^2} e^{-\frac{m_n^2+(a+br_n)^2}{2\sigma^2}} I_0\left(\frac{m_n(a+br_n)}{\sigma^2}\right). \tag{6}$$

Maximizing $\ln L$ with respect to (a, b, σ^2) yields the MLEs of a, b and σ^2 under H_1, denoted as $\widehat{\underline{a}}_1$, $\widehat{\underline{b}}$, and $\widehat{\underline{\sigma_1^2}}$, respectively.

3) *GLRT statistic*: The likelihood ratio test statistic is then given by

$$\underline{\lambda} = \frac{\sup\limits_{a,b,\sigma^2} L(a, b, \sigma^2; \underline{\boldsymbol{m}})}{\sup\limits_{a,\sigma^2} L(a, \sigma^2; \underline{\boldsymbol{m}})}. \tag{7}$$

The modified GLRT statistic $2 \ln \underline{\lambda}$ can then be written as

$$2 \ln \underline{\lambda} = 2 \sum_{n=1}^{N} \ln \frac{I_0\left(\frac{m_n \widehat{\underline{a}}_0}{\widehat{\underline{\sigma}_0^2}}\right)}{I_0\left(\frac{m_n(\widehat{\underline{a}}_1 + \widehat{\underline{b}} r_n)}{\widehat{\underline{\sigma}_1^2}}\right)} - \frac{N\widehat{\underline{a}}_0^2}{\widehat{\underline{\sigma}_0^2}} + \frac{1}{\widehat{\underline{\sigma}_1^2}} \sum_{n=1}^{N} (\widehat{\underline{a}}_1 + \widehat{\underline{b}} r_n)^2. \tag{8}$$

The test statistic (8) is asymptotically χ_1^2 distributed. The test will decide H_1 if and only if (8) exceeds a user specified threshold value η. In order to achieve a desired false alarm rate α, the threshold η can thus be chosen equal to $\chi^2_{1,1-\alpha}$, that is, the $(1-\alpha)$th quantile of the χ_1^2 distribution. The q^{th} quantile of the distribution of a continuous random variable $\underline{x}$ is defined as the smallest number η satisfying $Q_{\underline{x}}(\eta) = q$, with $Q_{\underline{x}}(x)$ the cumulative distribution function of $\underline{x}$ [18].

B. GLRTs for Complex fMRI Data

In this subsection, three different GLRTs for complex valued, Gaussian distributed data will be discussed. Thereby, it is assumed that we have N independent, complex data points $\boldsymbol{W} = (\boldsymbol{w}_r^T \boldsymbol{w}_i^T)$ of which the true (i.e., noiseless) components are described by $\boldsymbol{Z} = (\boldsymbol{z}_r^T \boldsymbol{z}_i^T)$, where

$$z_{r,n} = (a + br_n)\cos\varphi_n \tag{9}$$

$$z_{i,n} = (a + br_n)\sin\varphi_n \tag{10}$$

with φ_n denoting the n^{th} component of the $N \times 1$ deterministic phase vector $\boldsymbol{\varphi}$. For these data, the joint PDF of the complex data is simply the product of the real and imaginary PDFs and the likelihood function is given by

$$L = \left(\frac{1}{2\pi\sigma^2}\right)^N e^{-\frac{1}{2\sigma^2}\|\boldsymbol{z}_r - \boldsymbol{w}_r\|^2} e^{-\frac{1}{2\sigma^2}\|\boldsymbol{z}_i - \boldsymbol{w}_i\|^2}. \tag{11}$$

Note that this implies independence of the real and imaginary data. Taking the logarithm yields

$$\ln L = -N \ln(2\pi\sigma^2) - \frac{1}{2\sigma^2}\left(\|\boldsymbol{z}_r - \boldsymbol{w}_r\|^2 + \|\boldsymbol{z}_i - \boldsymbol{w}_i\|^2\right). \tag{12}$$

We now derive the MLEs of a, b, σ^2, and the parameters describing the phase vector $\boldsymbol{\varphi}$ in case the underlying true phase values $\{\varphi_n\}$ are identical, in case they are described by a linear model, and in case they are randomly distributed.

1) Identical Phase Values: Let c be the true phase of each complex data point

$$\boldsymbol{\varphi} = c\mathbf{1}. \tag{13}$$

a) *ML estimation under H_0*: Under H_0 (i.e., $b = 0$), the MLEs of a, c, and σ^2 are found by maximizing (12) with respect to (a, c, σ^2). For (a, c, σ^2) to be a maximum, the first order derivatives of the likelihood function with respect to a, c, and σ^2 should be zero. Solving the resulting system of equations yields the MLEs of a, c, and σ^2 under H_0 [25]:

$$\widehat{\underline{a}}_0 = \frac{1}{N}\sqrt{(\underline{\boldsymbol{w}}_r^T.\mathbf{1})^2 + (\underline{\boldsymbol{w}}_i^T.\mathbf{1})^2} \tag{14}$$

$$\widehat{\underline{c}}_0 = \arctan\frac{\underline{\boldsymbol{w}}_i^T.\mathbf{1}}{\underline{\boldsymbol{w}}_r^T.\mathbf{1}} \tag{15}$$

$$\begin{aligned}\widehat{\underline{\sigma}_0^2} &= \frac{1}{2N}\big(\|\widehat{\underline{a}}_0\cos\widehat{\underline{c}}_0\mathbf{1} - \boldsymbol{w}_r\|^2 \\ &\qquad + \|\widehat{\underline{a}}_0\sin\widehat{\underline{c}}_0\mathbf{1} - \boldsymbol{w}_i\|^2\big) \qquad (16)\\ &= \frac{1}{2N}\left(\left\|\left(\underline{\boldsymbol{w}}_r^T.\mathbf{1}\right)\mathbf{1} - \boldsymbol{w}_r\right\|^2\right. \\ &\qquad \left. + \left\|\left(\underline{\boldsymbol{w}}_i^T.\mathbf{1}\right)\mathbf{1} - \boldsymbol{w}_i\right\|^2\right). \qquad (17)\end{aligned}$$

b) *ML estimation under H_1:* Under H_1 (i.e., $b \neq 0$), maximizing $\ln L$ in (12) with respect to (a, b, c, σ^2) yields the following MLEs of a, b, c, and σ^2:

$$\widehat{\underline{a}}_1 = \frac{1}{N}\left[\left(\underline{\boldsymbol{w}}_r^T.\mathbf{1}\right)\cos\widehat{\underline{c}}_1 + \left(\underline{\boldsymbol{w}}_i^T.\mathbf{1}\right)\sin\widehat{\underline{c}}_1\right] \tag{18}$$

$$\widehat{\underline{b}} = \frac{1}{N}\left[\left(\underline{\boldsymbol{w}}_r^T.\boldsymbol{r}\right)\cos\widehat{\underline{c}}_1 + \left(\underline{\boldsymbol{w}}_i^T.\boldsymbol{r}\right)\sin\widehat{\underline{c}}_1\right] \tag{19}$$

$$\begin{aligned}\widehat{\underline{c}}_1 &= \frac{1}{2}\arctan \\ &\quad\times\frac{2\left(\left(\underline{\boldsymbol{w}}_r^T.\mathbf{1}\right)\left(\underline{\boldsymbol{w}}_i^T.\mathbf{1}\right)+\left(\underline{\boldsymbol{w}}_r^T.\boldsymbol{r}\right)\left(\underline{\boldsymbol{w}}_i^T.\boldsymbol{r}\right)\right)}{\left(\underline{\boldsymbol{w}}_r^T.\mathbf{1}\right)^2+\left(\underline{\boldsymbol{w}}_i^T.\mathbf{1}\right)^2+\left(\underline{\boldsymbol{w}}_r^T.\boldsymbol{r}\right)^2+\left(\underline{\boldsymbol{w}}_i^T.\boldsymbol{r}\right)^2}\end{aligned} \tag{20}$$

$$\begin{aligned}\widehat{\underline{\sigma}_1^2} &= \frac{1}{2N}\left(\left\|(\widehat{\underline{a}}_1\mathbf{1} + \widehat{\underline{b}}\boldsymbol{r})\cos\widehat{\underline{c}}_1 - \boldsymbol{w}_r\right\|^2\right. \\ &\qquad \left. + \left\|(\widehat{\underline{a}}_1\mathbf{1} + \widehat{\underline{b}}\boldsymbol{r})\sin\widehat{\underline{c}}_1 - \boldsymbol{w}_i\right\|^2\right).\end{aligned} \tag{21}$$

Note that no numerical optimization is required to find the MLEs (18)–(21).

c) *GLRT statistic*: From (11) and using the MLEs given in (14)–(21), a closed-form expression for the GLR can be obtained

$$\underline{\lambda} = \left(\frac{\widehat{\underline{\sigma}_0^2}}{\widehat{\underline{\sigma}_1^2}}\right)^N \tag{22}$$

with $\widehat{\underline{\sigma}_0^2}$ and $\widehat{\underline{\sigma}_1^2}$ given by (17) and (21), respectively. Furthermore, it can be shown that the test statistic

$$\underline{\kappa} = (2N-3)\left(\underline{\lambda}^{\frac{2}{2N}} - 1\right) = (2N-3)\left(\frac{\widehat{\underline{\sigma}_0^2}}{\widehat{\underline{\sigma}_1^2}} - 1\right) \tag{23}$$

is asymptotically $F_{1,2N-3}$-distributed under H_0 [24]. The test will decide H_1 if and only if the test statistic (23) exceeds a user specified threshold value. In order to achieve a specified false alarm rate α, this threshold should be chosen equal to $F_{1,2N-3,1-\alpha}$ (i.e., the $(1-\alpha)$th quantile of the $F_{1,2N-3}$ distribution). It should be mentioned that Nan and Nowak proposed $((N-1)/(2N-3))\underline{\kappa}$ as test statistic and $(1/2)F_{1,N-1,1-\alpha}$ as corresponding threshold, where the threshold was determined via Monte Carlo simulations [19]. Since it can be shown that for an increasing value of N, $((N-1)/(2N-3))F_{1,2N-3,1-\alpha}$ tends to $(1/2)F_{1,N-1,1-\alpha}$, both approaches are approximately equal. This has also been verified by means of simulations.

2) Linear Phase Model: Next, it is assumed that the true phase model is described by a constant baseline c on which an $N \times 1$ reference vector $\boldsymbol{s}$ with amplitude d is superimposed

$$\boldsymbol{\varphi} = c\mathbf{1} + d\boldsymbol{s}. \tag{24}$$

For example, $\boldsymbol{s}$ may be a linear trend or a reference function related to the employed paradigm.

a) *ML estimation under H_0*: Under H_0 (i.e., $b = 0$), the MLEs of a, c, d, and σ^2 are found by maximizing (12) with respect to (a, c, d, σ^2). In general, this is a four-dimensional optimization problem. However, by setting the first order derivatives with respect to a, c, and σ^2 to zero, closed-form expressions for the MLEs of a, c, and σ^2 can be obtained:

$$\widehat{\underline{a}}_0 = \frac{1}{N}\sum_{n=1}^{N}[\underline{w}_{r,n}\cos\widehat{\underline{\varphi}}_{0,n} + \underline{w}_{i,n}\sin\widehat{\underline{\varphi}}_{0,n}] \tag{25}$$

$$\begin{aligned}\widehat{\underline{c}}_0 &= \arctan \\ &\quad\times\frac{\sum_{n=1}^{N}\left[\underline{w}_{i,n}\cos(\widehat{\underline{d}}_0 s_n) - \underline{w}_{r,n}\sin(\widehat{\underline{d}}_0 s_n)\right]}{\sum_{n=1}^{N}\left[\underline{w}_{r,n}\cos(\widehat{\underline{d}}_0 s_n) + \underline{w}_{i,n}\sin(\widehat{\underline{d}}_0 s_n)\right]}\end{aligned} \tag{26}$$

$$\begin{aligned}\widehat{\underline{\sigma}_0^2} &= \frac{1}{2N}\sum_{n=1}^{N}\Big[(\widehat{\underline{a}}_0\cos\widehat{\underline{\varphi}}_{0,n} - w_{r,n})^2 \\ &\qquad + (\widehat{\underline{a}}_0\sin\widehat{\underline{\varphi}}_{0,n} - w_{i,n})^2\Big]\end{aligned} \tag{27}$$

where $\widehat{\underline{\varphi}}_{0,n} = \widehat{\underline{c}}_0 + \widehat{\underline{d}}_0 s_n$. To evaluate the MLEs given by (25)–(27), knowledge of the MLE $\widehat{\underline{d}}_0$ is required. It can be found by maximizing (12) with respect to d, under the constraints (25)–(27). Note that this is a one-dimensional optimization problem.

b) *ML estimation under H_1*: Under H_1 (i.e., $b \neq 0$), the MLEs of a, b, c, d, and σ^2 are found by maximizing (12) with respect to (a, b, c, d, σ^2). In general, this is a five-dimensional optimization problem. However, by setting the first order derivatives with respect to a, b, and σ^2 to zero, closed-form expressions for the MLEs of a, b, and σ^2 can be obtained

$$\widehat{\underline{a}}_1 = \frac{1}{N}\sum_{n=1}^{N}[\underline{w}_{r,n}\cos\widehat{\underline{\varphi}}_{1,n} + \underline{w}_{i,n}\sin\widehat{\underline{\varphi}}_{1,n}] \tag{28}$$

$$\widehat{\underline{b}} = \frac{1}{N}\sum_{n=1}^{N}[\underline{w}_{r,n}r_n\cos\widehat{\underline{\varphi}}_{1,n} + \underline{w}_{i,n}r_n\sin\widehat{\underline{\varphi}}_{1,n}] \tag{29}$$

$$\begin{aligned}\widehat{\underline{\sigma}_1^2} &= \frac{1}{2N}\sum_{n=1}^{N}\left[\left((\widehat{\underline{a}}_1 + \widehat{\underline{b}}r_n)\cos\widehat{\underline{\varphi}}_{1,n} - w_{r,n}\right)^2\right. \\ &\qquad \left. + \left((\widehat{\underline{a}}_1 + \widehat{\underline{b}}r_n)\sin\widehat{\underline{\varphi}}_{1,n} - w_{i,n}\right)^2\right]\end{aligned} \tag{30}$$

where $\widehat{\underline{\varphi}}_{1,n} = \widehat{\underline{c}}_1 + \widehat{\underline{d}}_1 s_n$. The MLEs given by (28)–(30) depend on the MLEs of c and d, of which no closed-form expression can be derived. Therefore, the latter estimators can only be obtained by maximizing (12) with respect to c and d, thereby using the constraints (28)–(30). Note that this is a 2-D optimization problem.

c) *GLRT statistic*: From (11) and using the MLEs given in (25)–(30), a closed-form expression for the GLR can be obtained

$$\underline{\lambda} = \left(\frac{\widehat{\underline{\sigma}_0^2}}{\widehat{\underline{\sigma}_1^2}} \right)^N \tag{31}$$

with $\widehat{\underline{\sigma}_0^2}$ and $\widehat{\underline{\sigma}_1^2}$ given by (27) and (30), respectively. Furthermore, it can be shown that the test statistic

$$\underline{\kappa} = (2N-4)\left(\underline{\lambda}^{\frac{2}{2N}} - 1\right) = (2N-4)\left(\frac{\widehat{\underline{\sigma}_0^2}}{\widehat{\underline{\sigma}_1^2}} - 1 \right) \tag{32}$$

is asymptotically $F_{1,2N-4}$-distributed under H_0. The test will decide H_1 if and only if the test statistic (32) exceeds a user specified threshold value. In order to achieve a specified false alarm rate α, this threshold should be chosen equal to $F_{1,2N-4,1-\alpha}$.

3) Random Phase Values: Next, let φ_n be the true phase of each complex data point.

a) *ML estimation under H_0*: Under H_0, b is zero. In that case, the MLEs for a, φ_n, and σ^2 are found by maximizing (12) with respect to a, φ_n, and σ^2. For (a, φ_n, σ^2) to be a maximum, the first order derivatives of the likelihood function with respect to a, φ_n, and σ^2 should be zero. Solving the resulting system then leads to the following MLEs under H_0 [25]:

$$\widehat{\underline{a}}_0 = \frac{1}{N} \underline{\boldsymbol{m}}^T . \mathbf{1} \tag{33}$$

$$\widehat{\underline{\varphi}}_{0,n} = \arctan\left(\frac{\underline{w}_{i,n}}{\underline{w}_{r,n}} \right) \tag{34}$$

$$\widehat{\underline{\sigma}_0^2} = \frac{1}{2N} \sum_{n=1}^{N} \left[(\widehat{\underline{a}}_0 \cos \widehat{\underline{\varphi}}_{0,n} - w_{r,n})^2 + (\widehat{\underline{a}}_0 \sin \widehat{\underline{\varphi}}_{0,n} - w_{i,n})^2 \right]. \tag{35}$$

Note that the MLEs given in (33)–(35) are simple closed-form expressions for which no numerical optimization is required.

b) *ML estimation under H_1*: Under H_1 (i.e., $b \neq 0$), the MLEs for a, b, φ_n, and σ^2 are then found by maximizing (12) with respect to a, b, φ_n, and σ^2. This leads to the following MLEs:

$$\widehat{\underline{a}}_1 = \frac{1}{N} \underline{\boldsymbol{m}}^T . \mathbf{1} \tag{36}$$

$$\widehat{\underline{b}} = \frac{1}{N} \underline{\boldsymbol{m}}^T . \boldsymbol{r} \tag{37}$$

$$\widehat{\underline{\varphi}}_{1,n} = \arctan\left(\frac{\underline{w}_{i,n}}{\underline{w}_{r,n}} \right) \tag{38}$$

$$\widehat{\underline{\sigma}_1^2} = \frac{1}{2N} \sum_{n=1}^{N} \left[\left((\widehat{\underline{a}}_1 + \widehat{\underline{b}} r_n) \cos \widehat{\underline{\varphi}}_{1,n} - w_{r,n} \right)^2 + \left((\widehat{\underline{a}}_1 + \widehat{\underline{b}} r_n) \sin \widehat{\underline{\varphi}}_{1,n} - w_{i,n} \right)^2 \right] \tag{39}$$

Note that also in this case the MLEs given in (36)–(39) are simple closed-form expressions for which no numerical optimization is required.

c) *GLRT statistic*: From (11) and using the MLEs given in (33)–(39), a closed-form expression for the GLR can be obtained

$$\underline{\lambda} = \left(\frac{\widehat{\underline{\sigma}_0^2}}{\widehat{\underline{\sigma}_1^2}} \right)^N \tag{40}$$

with $\widehat{\underline{\sigma}_0^2}$ and $\widehat{\underline{\sigma}_1^2}$ given by (35) and (39), respectively. Furthermore, it can be shown that the test statistic

$$\underline{\kappa} = (N-2)\left(\underline{\lambda}^{\frac{2}{2N}} - 1\right) = (N-2)\left(\frac{\widehat{\underline{\sigma}_0^2}}{\widehat{\underline{\sigma}_1^2}} - 1 \right) \tag{41}$$

is asymptotically $F_{1,N-2}$-distributed under H_0. The test will decide H_1 if and only if the test statistic (41) exceeds a user specified threshold value. In order to achieve a specified false alarm rate α, this threshold should be chosen equal to $F_{1,N-2,1-\alpha}$. Note that this test is identical to the well-known generalized linear model test applied to magnitude data [6].

IV. Simulation Results and Discussion

Monte Carlo simulation experiments were set up to compare the performance of the GLRT for magnitude data to the performance of the GLRTs based on complex data. The test's performances were evaluated in terms of the CFAR property and the detection rate P_d. For this purpose, numerous realizations of fMRI time series were generated of which the noiseless real and imaginary components are described by (9) and (10), respectively. As a reference function, a square wave was considered, which fluctuates between -1 and $+1$ with period 20. Three phase models were considered: a constant phase model, a linear phase model, and a random phase model. For the linear phase model, a slope of 0.01 rad/point was applied. This is comparable with the slope observed from experimental fMRI data (see, e.g., Fig. 1). For the random phase model, the true phases were generated using a uniform random generator in the interval $[-\pi, \pi]$. Gaussian distributed, zero mean noise with variance σ^2 was added to the noiseless, complex data. Hence, the magnitude data sets obtained from the complex data sets were Rician distributed.

A. CFAR Property

First, simulation experiments have been run so as to find out to what extent the tests under concern have the CFAR property. The reason for this is that tests that do not have the CFAR property are of little practical use, since the SNR is usually unknown beforehand. Although it is known that the GLRT has the CFAR

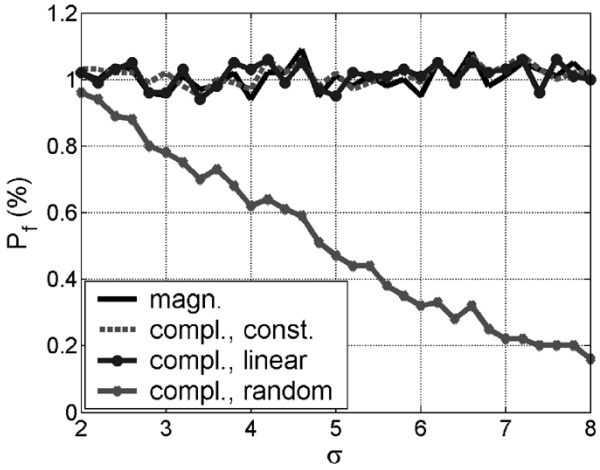

Fig. 2. False alarm rate as a function of the noise standard deviation σ ($a = 10$, $P_f = 0.01$). Results are shown for the GLRT based on magnitude data and for the GLRTs based on complex data and constant, linear and random phase model. The true phases were constant. Note that only the GLRT based on complex data and a random phase model does not have the CFAR property.

property asymptotically, it remains to be seen whether this property still applies to a finite number of observations.

For all tests, the threshold was set to $\chi^2_{1,0.99}$, that is, the 99% quantile of the χ^2_1 distribution. For each point, a sample size of 10^6 was employed. The simulation results for the CFAR property of the GLRTs can be summarized as follows.

- For numbers of observations that are representative of those available in practical fMRI measurements, the GLRT based on the magnitude data has the CFAR property, at least for $\mathrm{SNR} > 1$. Of course, this holds for any underlying phase model since the GLRT based on magnitude data is not influenced by the underlying phases.
- The GLRT based on complex data and constant phases, as well as the GLRT based on complex data and a linear phase model was observed to have the CFAR property as long as the true, underlying phases were constant or described by the correct linear model, respectively. In general, as long as the true phase variations are correctly described by the imposed phase model, the CFAR property should hold.
- Alternatively, from the simulation results it was also clear that, if the true underlying phases were not described by an appropriate model, the CFAR property did not hold. For example, the GLRT based on complex data and constant phases did not have the CFAR property when applied to data described by a linear phase model in which the model parameter d was different from zero.
- Finally, the GLRT based on complex data and random phases was observed to lack the CFAR property (see Fig. 2). This may seem remarkable since any underlying phase model can be correctly modeled by a random phase model. However, the lack of CFAR property may be explained by the fact that for a random phase model the number of estimated parameters is very large in comparison with the number of data points [14].

These results, summarized in Table I, indicate that, for a very wide range of SNRs (simulations were run for SNRs larger than 1), a GLRT for magnitude data holds the CFAR property. On the other hand, when the phase model used in a GLRT based on complex data does not describe the underlying phases in an appropriate way, such a GLRT does not have the CFAR property and is therefore of little use in practice. In the following subsection, the GLRTs that do have the CFAR property are compared with respect to detection rate.

B. Detection Rate

For GLRTs that have the CFAR property, simulation experiments were run to test the detection rate. Thereby, for a fixed false alarm rate P_f, the detection rate P_d was determined as a function of the noise standard deviation (sample size was 10^5, $a = 10$, $N = 120$). In each experiment, the threshold was set to $\chi^2_{1,0.99}$. For truly χ^2_1 distributed test statistics, this would lead to a false alarm rate $P_f = 0.01$, which is a representative value of the P_f values used in fMRI.

The results obtained from the experiments showed that for low values of the SNR the detection rates for GLRTs based on complex data were significantly higher than the detection rates for the GLRT based on magnitude data, at least as long as the phase model was correctly specified. In particular, when the true phases were constant, it was noted that for low SNR

- the detection rate of the GLRT for complex data and constant phases was significantly higher than the GLRT for complex data and a linear phase model;
- the detection rate of the GLRT for complex data and a linear phase model was significantly higher than the GLRT for magnitude data.

This is shown in Fig. 3. It shows the detection rates as a function of the noise standard deviation σ for the GLRT for magnitude data and the GLRT for a constant and linear phase model. For very small values of σ, i.e., at high SNR, the detection rates do not differ significantly. For increasing values of σ, the difference in detection rate between the GLRTs increases. From Fig. 3, it is clear that the GLRT based on a constant phase model performs best with respect to detection rate. Note, however, that this is a very specific case, i.e., when the underlying phases are constant and a GLRT for complex data and a constant phase model is applied.

Whenever a GLRT for complex data is applied based on a more advanced phase model, the difference between the detection rate of this GLRT and the detection rate of a GLRT based on magnitude data drops significantly. Indeed, it seems that, with an increasing number of phase model parameters, the detection rate of the GLRT based on complex data decreases significantly. This can also be concluded from Fig. 3. The detection rate for the GLRT based on complex data and a linear phase model (which also correctly models constant phases) is comparable to the detection rate of a GLRT based on magnitude data for a larger range of SNRs. Hence, it is clear that the addition of even a single phase parameter significantly lowers the detection rate of the GLRT based on complex data. Although no GLRT for complex data was constructed that had more than two phase parameters, it is expected that the detection rate of such a GLRT would hardly be any different from the detection rate of a GLRT for magnitude data.

TABLE I
CFAR PROPERTY OF THE GLRTS FOR CONSTANT PHASES, LINEARLY VARYING PHASES (WITH STEP $\Delta\varphi$), AND RANDOM PHASES. IF A GLRT HOLDS THE CFAR PROPERTY, THIS IS DENOTED BY ✓

	GLRT magnitude data	GLRT complex data constant phase model	GLRT complex data linear phase model	GLRT complex data random phase model
$\varphi_n = \varphi$	✓	✓	✓	-
$\varphi_n = \varphi + n\Delta\varphi$	✓	-	✓	-
$\varphi_n =$ random	✓	-	-	-

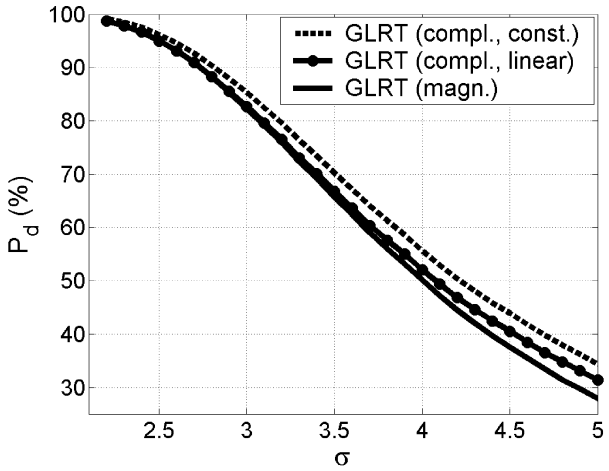

Fig. 3. Detection rates as a function of the noise standard deviation σ ($a = 10$, $P_f = 0.01$). Results are shown for the GLRT based on magnitude data, for the GLRT based on complex data and constant phases, and for the GLRT based on complex data with a linear phase model. The true phases were constant.

V. CONCLUSION

Most statistical tests for detecting activation from functional fMRI data are applied to the magnitude components of intrinsically complex valued fMRI data. However, previous work has reported the observation that the phase components of an fMRI time course are virtually constant. Based on this observation, a generalized likelihood ratio test (GLRT) for complex valued fMRI data with constant phases was developed, showing significantly higher detection rates compared to standard tests in low SNR regions [19].

However, phase values of complex fMRI time series may not be constant but for example linearly varying or related to the paradigm. Therefore, in this work, we tested the performance of the GLRT based on constant phases if a slight nonconstant behavior was introduced to the phase components. Simulation results show that, even with a small deviation from a constant baseline, the detection rate of this GLRT drops drastically, and, even worse, the GLRT looses its constant false alarm rate (CFAR) property. Hence, we conclude that a GLRT based on complex data and constant phases is very vulnerable to a misspecification of the phase model underlying the complex fMRI data.

Furthermore, a GLRT for complex data with a linear phase model was constructed. Such a test covers a much wider range of phase models, but requires the estimation of an additional parameter. It was shown that, whenever the underlying phase model was correct, this GLRT showed a slight improvement of detection rate compared to a GLRT based on magnitude data and was observed to have the CFAR property. In case the underlying phases could not be described by a linear phase model, the performance of this GLRT was observed to drop drastically as well.

In conclusion, we believe that in practice it is safer to use a GLRT for magnitude fMRI data than a GLRT for complex fMRI data, unless one is absolutely confident that the underlying phase values are constant.

REFERENCES

[1] J. Belliveau, D. N. Kennedy, R. McKinstry, B. Buchbinder, R. Weisskoff, M. Cohen, J. Vevea, T. Brady, and B. Rosen, "Functional mapping of the human visual cortex by magnetic resonance imaging," *Science*, vol. 254, no. 5032, pp. 716–719, 1991.

[2] M. A. Burock and A. M. Dale, "Estimation and detection of fMRI event-related signals: a statistically efficient and unbiased approach," *Hum. Brain. Mapp*, vol. 11, pp. 249–260, 2000.

[3] V. D. Calhoun, T. Adali, G. D. Pearlson, P. van Zijl, and J. J. Pekar, "Independent component analysis of fMRI data in the complex domain," *Magn. Reson. Med.*, vol. 48, pp. 180–192, 2002.

[4] M. Desco, J. A. Hernandez, A. Santos, and M. Brammer, "Multiresolution analysis in fMRI: sensitivity and specificity in the detection of brain activation," *Hum. Brain. Mapp*, vol. 14, no. 1, pp. 16–27, 2001.

[5] K. J. Friston, P. Fletcher, O. Josephs, A. Holmes, M. D. Rugg, and R. Turner, "Event-related fMRI: characterizing differential responses," *NeuroImage*, vol. 7, pp. 30–40, 1998.

[6] K. J. Friston, P. Jezzard, and R. Turner, "Analysis of functional MRI time series," *Hum. Brain. Mapp*, vol. 1, pp. 153–171, 1994.

[7] G. H. Glover, T. Li, and D. Ress, "Image-based method for retrospective correction of physiological motion effects in fMRI: RETROICOR," *Magn. Reson. Med.*, vol. 44, pp. 162–167, 2000.

[8] H. Gudbjartsson and S. Patz, "The Rician distribution of noisy MRI data," *Magn. Reson. Med.*, vol. 34, pp. 910–914, 1995.

[9] P. G. Hoel, S. C. Port, and C. J. Stone, *Introduction to Statistical Theory*. New York: Houghton Mifflin, 1971.

[10] F. G. Hoogenraad, J. R. Reichenbach, E. M. Haacke, S. Lai, K. Kuppusamy, and M. Sprenger, "In vivo measurement of changes in venous blood-oxygenation with high resolution functional MRI at 0.95 tesla by measuring changes in susceptibility and velocity," *Magn. Reson. Med.*, vol. 39, pp. 97–107, 1998.

[11] S. M. Kay, *Fundamentals of Statistical Signal Processing, Volume II Detection Theory*. Upper Saddle River, NJ: Prentice Hall PTR, 1998.

[12] S. J. Kisner and T. M. Talavage, "Testing the distribution of non-stationary MRI data," in *Proc. 26th Int. Conf. IEEE Engineering in Medicine and Biology Society*, San Francisco, CA, Sep. 1–5, 2004, no. 1054.

[13] S. J. Kisner, T. M. Talavage, and J. L. Ulmer, "Testing a model for MR imager noise," in *Proc. 2nd Joint EMBS-BMES Conf.*, vol. 2, Houston, TX, Oct. 23–26, 2002, pp. 1086–1087.

[14] L. Lebart, A. Morineau, and M. Piron, *Statistique exploratoire multidimensionnelle*. Paris, France: Dunod, 2000.

[15] W.-L. Luo and T. E. Nichols, "Diagnosis and exploration of massively univariate neuroimaging models," *NeuroImage*, vol. 19, no. 3, pp. 1014–1032, 2003.

[16] M. J. McKeown, S. Makeig, G. B. Brown, T.-P. Jung, S. S. Kindermann, A. J. Bell, and T. J. Sejnowski, "Analysis of fMRI data by blind separation into independent spatial components," *Hum. Brain. Mapp*, vol. 6, pp. 160–188, 1998.

[17] R. S. Menon, "Postacquisition suppression of large-vessel BOLD signals in high-resolution fMRI," *Magn. Reson. Med.*, vol. 47, pp. 1–9, 2002.

[18] A. M. Mood, F. A. Graybill, and D. C. Boes, *Introduction to the Theory of Statistics*, 3rd ed. Tokyo, Japan: McGraw-Hill, 1974.

[19] F. Y. Nan and R. D. Nowak, "Generalized likelihood ratio detection for fMRI using complex data," *IEEE Trans. Med. Imag.*, vol. 18, no. 4, pp. 320–329, Apr. 1999.

[20] S. M. Rao, J. R. Binder, P. A. Bandettini, T. A. Hammeke, Z. A. Yetkin, J. Jesmanowicz, L. M. Lisk, G. L. Morris, W. M. Mueller, L. D. Estkowski, E. C. Wong, V. M. Haughton, and J. S. Hyde, "Functional magnetic resonance imaging of complex human movements," *Neurology*, vol. 43, pp. 2311–2318, 1993.

[21] D. B. Rowe and B. R. Logan, "A complex way to compute fmri activation," *Neuroimage*, vol. 23, no. 3, pp. 1078–1092, Nov. 2004.

[22] S. Ruan, C. Jaggi, J. M. Constans, and D. Bloyet, "Detection of brain activation from MRI data by likelihood-ratio test," in *Proc. 1st Int. Conf. Computer Vision, Virtual Reality and Robotics in Medicine*, 1995, pp. 341–350.

[23] W. Schneider, D. C. Noll, and J. D. Cohen, "Functional topographic mapping of the cortical ribbon in human vision with conventional MRI scanners," *Nature*, vol. 365, pp. 150–153, 1993.

[24] G. A. F. Seber and C. J. Wild, *Nonlinear Regression*. New York: Wiley, 1989.

[25] J. Sijbers and A. J. den Dekker, "Maximum likelihood estimation of signal amplitude and noise variance from MR data," *Magn. Reson. Med.*, vol. 51, no. 3, pp. 586–594, 2004.

[26] J. Sijbers, A. J. den Dekker, E. Raman, and D. Van Dyck, "Parameter estimation from magnitude MR images," *Int. J. Imag. Syst. Tech.*, vol. 10, no. 2, pp. 109–114, 1999.

[27] J. V. Stone, "Independent component analysis: an introduction," *Trends Cogn. Sci.*, vol. 6, no. 2, pp. 59–64, 2002.

[28] N. Vanello, V. Positano, E. Ricciardi, M. F. Santarelli, M. Guazzelli, P. Pietrini, and L. Landini, "Separation of movement and task related fMRI signal changes in a simulated data set by independent component analysis," *NeuroImage*, vol. 19, no. 2, p. 968, 2003.

[29] M. W. Woolrich, B. D. Ripley, J. M. Brady, and S. Smith, "Temporal autocorrelation in univariate linear modeling of fMRI data," *NeuroImage*, vol. 14, no. 6, pp. 1370–1386, 2001.

[30] K. J. Worsley, C. H. Liao, J. Aston, V. Petre, G. H. Duncan, F. Morales, and A. C. Evans, "A general statistical analysis for fMRI data," *NeuroImage*, vol. 15, pp. 1–15, 2002.

[31] J. Zigun, J. Frank, F. A. Barrios, D. W. Jones, T. K. F. Foo, C. T. W. Moonen, D. Z. Press, and D. R. Weinberger, "Measurement of brain activity with bolus administration of contrast agent and gradient-echo MR imaging," *Radiology*, vol. 186, no. 2, pp. 353–356, 1993.